Self-propagating high temperature synthesis and dynamic compaction of titanium diboride/titanium carbide composites

I. SONG, L. WANG, M. WIXOM
T/J Technologies, Inc., Ann Arbor, MI 48106, USA

L. T. THOMPSON
University of Michigan, Department of Chemical Engineering, Ann Arbor, MI 48109-2136, USA
E-mail: ltt@umich.edu

Self-propagating High-temperature Synthesis (SHS) of titanium and boron carbide (B_4C) combined with explosively driven Dynamic Compaction (DC) was employed for the fabrication of composite TiB_2/TiC compacts. A 2^3 factorially designed experiment set was used to examine the effects of the TiB_2/TiC ratio, delay time and C/M ratio on the consolidation and properties of the compacts. The delay time is the time between completion of the SHS reaction and compaction. The C/M ratio, the ratio of the explosive mass to that of the flyer plate, influences the pressure applied to the samples during compaction. Composites with molar TiB_2/TiC ratios of 2 : 1 or 1 : 2 were prepared using Ti and B_4C or Ti, C and B_4C, respectively, as reactants. The SHS/DC of Ti and B_4C resulted in high quality, near fully dense TiB_2/TiC composite compacts. Under best conditions, the densities were greater than 98% of the theoretical maximum. While the microhardness and densities of the compacts with TiB_2/TiC ratio of 2 : 1 were comparable to those of monolithic TiB_2 and TiC, compacts with TiB_2/TiC ratios of 1 : 2 were poorly consolidated and contained extensive cracks. Given the high energy and time efficiency, high product quality and inexpensive reactants, the SHS/DC of Ti and B_4C represents an attractive technique for the economical fabrication of TiB_2/TiC composites. © *2000 Kluwer Academic Publishers*

1. Introduction

Titanium diboride and titanium carbide are attractive for application in aircraft propulsion systems and space vehicle thermal protection systems because of their high melting point, good thermal shock resistance, excellent high-temperature stability, and light weight. They are also potential candidates for applications in cutting tools, wear-resistant parts, and armored vehicles [1–3].
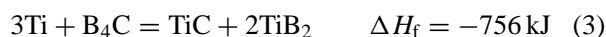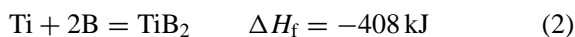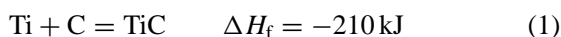
Fabrication of TiB_2 and TiC ceramics by conventional sintering, hot-pressing or hot-isostatic pressing (HIP) is costly because of the time-intensive and facility-intensive nature of these processes. The application of TiB_2 and TiC ceramics has thus been limited. Self-propagating high-temperature synthesis (SHS) combined with dynamic compaction, however, provides a new method for producing TiB_2 and TiC ceramics. The SHS process takes advantage of the extreme heat generated during the formation of refractory materials. When a compact of the constituent elements is ignited at one end, the highly exothermic reaction propagates spontaneously and rapidly, converting the reactants into a refractory product. The reaction temperature can exceed 2500 °C. This technique has attracted

attention as a route to a variety of refractory materials including borides, carbides, nitrides, silicides and intermetallic compounds [4–6]. The SHS technique has advantages: (1) high energy and time efficiency, and (2) high product purity due to the expulsion of volatile contaminates as a result of the extremely high temperatures. The SHS products, however, cannot be used directly as structural materials because they are generally quite porous (the porosity can be as high as 50 vol%). In order to make dense bodies, the SHS-prepared materials must be further processed. Several compaction techniques have been employed in combination with SHS.

The dynamic compaction (DC) technique was demonstrated to be an effective method for densifying highly refractory materials including TiB_2 and TiC [7, 8]. We have found, however, several limitations associated with the SHS/DC fabrication of pure TiC and TiB_2. Severe cracks were often observed in the TiC compacts. Low heat of formation, low reaction temperature and high thermal expansion coefficient of TiC were considered to be the major reasons for the cracking [9, 10]. The low reaction temperature would result in a low plasticity, and high thermal expansion would cause significant stresses across the compact during

cooling. On the other hand, the very high reaction heat released during the formation of pure TiB_2 can cause cracking and failure of the container. It is expected that the simultaneous formation of TiB_2 and TiC in a TiB_2/TiC composite would mitigate the problems associated with the fabrication of monolithic TiB_2 and TiC. There are other potential advantages to the production of TiB_2/TiC composites. The production of TiB_2/TiC via SHS/DC of elemental Ti, B and C is costly due to the very high cost of boron powder. A plausible solution to this problem is a fabrication of TiB_2/TiC composites using B_4C as a reactant. Boron carbide is at least 5 times less expensive than boron. Using B_4C instead of pure boron and carbon, the raw material costs for producing TiB_2/TiC composites could be reduced by almost 75%.

The feasibility of using B_4C to replace (or partially replace) boron and carbon can be understood using related thermodynamic data [11]. For example, at 2500 °C,

$$\text{Ti} + \text{C} = \text{TiC} \qquad \Delta H_f = -210\,\text{kJ} \qquad (1)$$

$$\text{Ti} + 2\text{B} = \text{TiB}_2 \qquad \Delta H_f = -408\,\text{kJ} \qquad (2)$$

$$3\text{Ti} + \text{B}_4\text{C} = \text{TiC} + 2\text{TiB}_2 \qquad \Delta H_f = -756\,\text{kJ} \quad (3)$$

Considering the fact that three moles of product are formed in reaction (3), the average reaction heat is -252 kJ/mole, $\sim$25% higher than that of reaction (1) and significantly less than that of reaction (2). The SHS of TiB_2/TiC using B_4C and Ti reactants was first demonstrated by McCauley et al. [12]. The major objective of work described in this paper was to examine the effects of several processing parameters on the consolidation and properties of the TiB_2/TiC compacts.

2. Experimental

2.1. Experimental design

The effects of the target TiB_2 : TiC ratio, delay time and C/M ratio were investigated. The delay time is the time between completion of the SHS reaction and compaction. It affects the sample temperature and hence the plasticity during compaction. The C/M ratio is the ratio of the mass of the explosive to that of the flyer plate and reflects the flyer plate velocity indirectly. Higher flyer plate velocities subject the samples to higher pressures upon impact. Orthogonally designed experiments were carried out to examine the effects of these parameters on the consolidation and properties of TiB_2/TiC compacts. Two levels for each of the three factors were examined. The two levels for the Ti : C : B_4C molar ratio were 3 : 0 : 1 and 6 : 3 : 1, corresponding to TiB_2/TiC target ratios of 2 : 1 and 1 : 2. Previously a C/M ratio of 0.2 was used for TiB_2, and C/M ratios of 0.4 and 0.6 for TiC [7, 8]. Considering the fact that the heat generated by reaction (3) is closer to that of reaction (1), C/M ratios of 0.3 and 0.6 were used for the TiB_2/TiC composites. Previous results showed that delay times of 5 sec were adequate for both TiC and TiB_2 [7, 8]. In this study, delay times of 5 and 10 sec were tested for the TiB_2/TiC composites.

TABLE I Experimental conditions for self propagating high temperature synthesis/dynamic compaction experiments

Compact	Composition % (wt)			Delay (sec)	C/M ratio
	Ti	B_4C	C		
TJ01	72.2	27.8		5	0.3
TJ02	72.2	27.8		5	0.6
TJ03	72.2	27.8		10	0.3
TJ04	72.2	27.8		10	0.6
TJ05	75.9	14.6	9.5	5	0.3
TJ06	75.9	14.6	9.5	5	0.6
TJ07	75.9	14.6	9.5	10	0.3
TJ08	75.9	14.6	9.5	10	0.6

A series of 8 experiments was carried out as indicated in Table I. The experimental results were analyzed using standard procedures for the statistical analysis of 2^k factorially designed experiments.

2.2. Synthesis

The raw materials were titanium (99.5%, -325 mesh; Micro Metals), boron carbide (99.9%, -325 mesh; Alfa), and carbon (99.9%, 2 μm; Consolidated Astronautics) powders. The appropriate amounts of each powder were dry mixed under an argon atmosphere for 12 hours using a V-shaped plastic mechanical blender. The mixture was uniaxially pressed using a hydraulic press into greenforms $\sim$100 mm in diameter and $\sim$40 mm in thickness with a green density of $\sim$60%.

The experimental set-up is illustrated in Fig. 1. The system consisted of layers of gypsum wallboard which were center-cored to a diameter slightly larger than the greenforms. Two telescoping, mild steel rings of equal height were placed between the greenform and the gypsum to serve as lateral containment during the reaction and subsequent compaction. The bottom ring and the gypsum block had four matching holes to vent gases
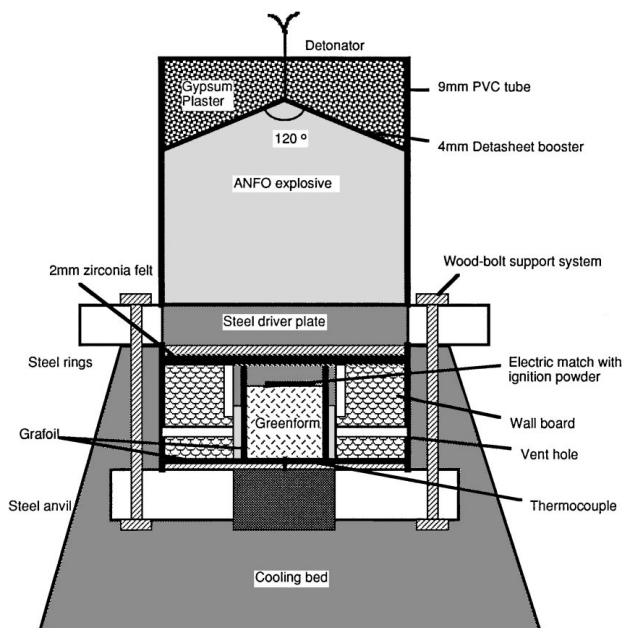

Figure 1 Schematic of the set-up for the SHS/DC experiments.

released during the reaction. A Grafoil strip was placed between the steel ring and the greenform to provide thermal insulation and prevent impurities from diffusing into the reacted compact. Circular driver plates and momentum traps of high hardness steel (MIL SPEC 46100) were epoxied into wooden frames, and lined with zirconia felt and Grafoil sheet. The explosive loading assembly consisted of a PVC tube into which a 120° gypsum cone was cast. The apex of the cone was lined to a density of 0.9 g/cm^3 yielding a detonation velocity of 3480 m/s. Such a cone-initiated explosive charge provides a plane wave to the flyer plate and generates a uniform pressure loading onto the sample for a uniform compaction.

The reactants were ignited using an electric match through a loose ignition powder seated on top of the sample. The reaction propagated downward through the entire sample. The explosive was detonated upon completion of the reaction which was verified with a thermocouple located at the bottom of the sample.

2.3. Characterization

Samples for analysis were cut using a diamond saw from different areas of the compacts to examine the uniformity of the microstructure and mechanical properties. The samples were analyzed for density, phase constituents, microstructure and microhardness.

Density was measured for specimens cut from the central region using an Archimedean method. Previously we found that density was uniform across the compact. The specimen was boiled in water for at least 2 hour to ensure that all open pores were filled with water. The displacement of water was used to calculate the volume of the specimen. The theoretical densities were calculated based on the target compositions. The phase constituents in the SHS reacted and explosively densified compacts were examined by x-ray diffraction (XRD). Specimens for microstructural analysis were polished sequentially using diamond pastes with grit sizes of 45, 30, 15, 6 and 1 μm. The polished samples were etched using a solution of 2 parts HNO_3, 1 part CH_3COOH, and 1 part HF. The microstructure was examined using scanning electron microscopy (SEM). Grain sizes were determined using the linear intercept technique devised by Mendelson according to the following equation [13]:

$$D = 1.57\,C/(NM) \qquad (4)$$

where, D is the grain size, C the length of the test line, N the number of grain boundary intercepts and M the magnification of the micrograph. The proportionality constant, 1.57, relates the average grain size to the average intercept length of a random section through a space-filling array of grains. At least four micrographs were taken from each area in the compact. The microhardness was measured using a Knoop hardness tester. The hardness tests were performed on specimens from several different areas in the compact to examine the effect of microstructure on hardness. Between 20 to 30 indentations were made in each area to obtain a statis-

tically significant result. The effect of grain boundary strength on hardness was also examined by increasing the applied load.

3. Results
3.1. Physical appearance and density
The SHS reacted and explosively compressed compacts with a TiB_2/TiC molar ratio of 2 : 1 were recovered as single piece plates of 100 mm diameter and 20 mm thickness. The surfaces were smooth with no major cracks although some edge delamination occurred. This is in contrast to the monolithic TiC and TiB_2 compacts that we fabricated in earlier studies [1, 2]. The monolithic compacts contained two types of cracks; large cracks often going through the compacts, and smaller cracks with much higher number densities. Cracking of the TiC compacts was attributed to its low heat of formation and high coefficient of thermal expansion. One of the reasons for cracking of the monolithic TiB_2 compacts could be the very high reaction heat which could cause failure of the steel container. Our results showed that the combination of TiB_2 and TiC was effective for producing high quality Ti-based ceramic compacts.

Compacts TJ01, TJ02, TJ03 and TJ04 were consolidated to greater than 98% of the theoretical density. These densities are comparable to the highest values achieved for monolithic TiB_2 (99.3%) and TiC (96.8%) [7, 8]. The densities for all four compacts were quite consistent (see Table II). The results indicated that a C/M ratio of 0.3–0.6, and a delay time of 5–10 sec were adequate for greater than 98% compaction of the $TiB_2/TiC = 2 : 1$ composites. Within these ranges, neither factor had a significant effect on the density. This observation may be explained based on the calculated values for the impact velocities and energy input during SHS/DC. Using a delay time of 5 seconds instead of 10 seconds would only increase the temperature by ~100 °C based on a two dimensional simulation of the SHS/DC of TiC [9].

The reactant composition had a very significant effect on the properties of the compacts. The compacts with a TiB_2/TiC molar ratio of 1 : 2 were recovered as single piece, loosely compacted plates of ~110 mm diameter and ~20 mm thickness, or several broken pieces with cracks. While the impact surfaces were relatively smooth, the non-impact surfaces had extensive cracks. Compared to the compacts with TiB_2/TiC molar ratios of 2 : 1 (TJ01, TJ02, TJ03, and TJ04), the compacts with

TABLE II Densities of TiB_2/TiC composites

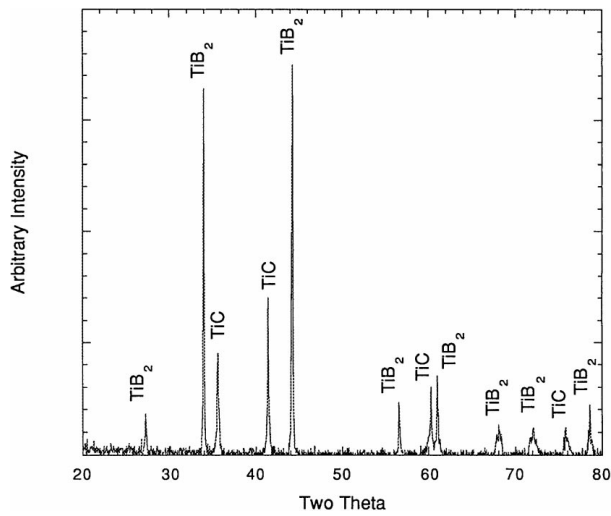| Compact	C/M ratio	Delay time (sec)	TiB_2/TiC (molar ratio)	Density (g/cm^3)	(% Theoretical)
TJ01	0.3	5	2 : 1	4.557	98.3
TJ02	0.6	5	2 : 1	4.568	98.5
TJ03	0.3	10	2 : 1	4.576	98.7
TJ04	0.6	10	2 : 1	4.561	98.4
TJ05	0.3	5	1 : 2	4.072	85.2
TJ06	0.6	5	1 : 2	3.948	82.6
TJ07	0.3	10	1 : 2	4.086	85.5
TJ08	0.6	10	1 : 2	4.087	85.5

Figure 2 X-ray diffraction pattern of a TiB$_2$-rich composite compact (TJ01).

molar ratios of $1:2$ (TJ05, TJ06, TJ07 and TJ08) suffered from severe edge delamination, extensive cracking, and lower densities. Since the overall appearances of the compacts with a TiB$_2$/TiC molar ratio of $1:2$ were uniform and the x-ray diffraction patterns contained well defined peaks of TiB$_2$ and TiC with no evidence of residual B$_4$C, Ti, or C, we concluded that these

compacts reacted uniformly. Thus, the extensive cracking was not likely caused by incomplete reaction, or by improper selection of the delay time, or C/M ratio. Instead we believe that the primary difference was due to differences in the heats of reaction. The heat of reaction is a sensitive function of the compact composition.

3.2. Phase constituents and microstructures

X-ray diffraction patterns for the TJ01, TJ02, TJ03 and TJ04 compacts were similar. Fig. 2 shows the x-ray diffraction pattern for the TJ01 compact. All the compacts contained TiB$_2$ and TiC with no peaks indicative of unreacted B$_4$C or elemental Ti. The TiB$_2$ peaks were more intense than those for TiC. This was expected given the reactant compositions. Fig. 3 shows typical scanning electron micrographs of compacts TJ01, TJ02, TJ03 and TJ04. All revealed well bonded grains and a relatively uniform composite structure, free of porosity. The dark elongated grains are TiB$_2$, whereas the irregular but more equiaxed grains are TiC. The grain shapes were similar to those observed for monolithic TiB$_2$ and TiC [7, 8]. Ten lines were drawn randomly on each micrograph to determine the average grain sizes. The average grain size was obtained from over 40 line-measurements that intercepted several hundred grains and therefore provided
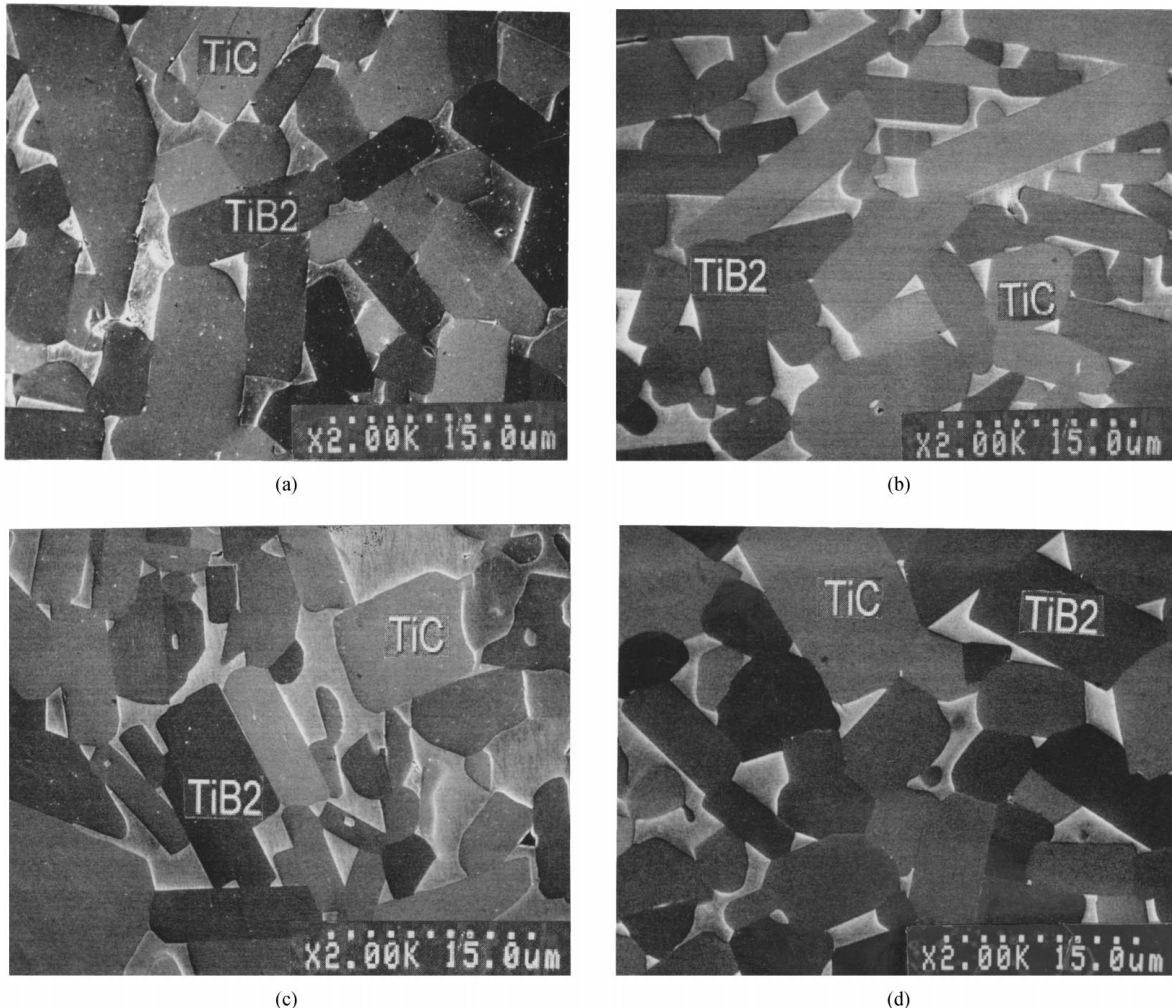

Figure 3 Scanning electron micrographs of the TiB$_2$/TiC compacts prepared by SHS/DC; (a) TJ01, (b) TJ02, (c) TJ03 and (d) TJ04.

TABLE III Average grain sizes for TiB_2/TiC composites

Compact	Average grain size (μm)
TJ01	3.6 ± 0.4
TJ02	3.4 ± 0.3
TJ03	3.9 ± 0.5
TJ04	4.2 ± 0.6

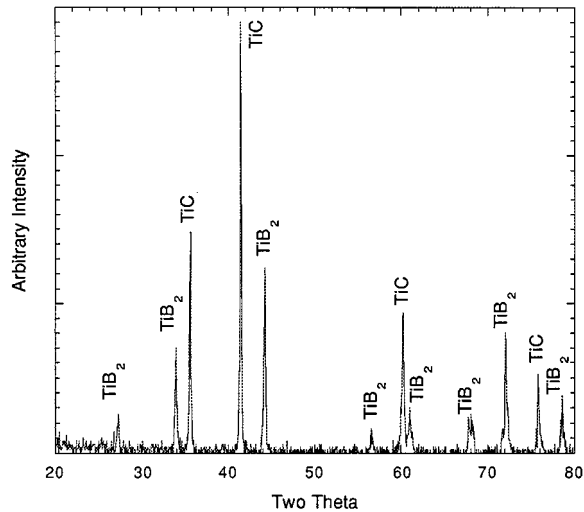*Figure 5* Effect of test load on the measured hardness.

Figure 4 X-ray diffraction pattern of a TiC-rich composite compact (TJ05).

a statistically reliable value. The average grain sizes for TJ01, TJ02, TJ03 and TJ04 are given in Table III. The grain sizes were very similar. These grain sizes were considerably smaller than those of monolithic TiB_2 and TiC compacts that we previously prepared [7, 8].

Fig. 4 shows the x-ray diffraction pattern for the TJ05 compact. The TJ06, TJ07 and TJ08 compacts yielded similar patterns. All of the compacts contained TiB_2 and TiC with no evidence of unreacted B_4C, elemental C or Ti. Unlike the 2 : 1 molar ratio of compacts, the TiC peaks were more intense than the TiB_2 peaks. This observation is again consistent with the reactant compositions. The 1 : 2 molar ratio compacts contained macro voids, and were quite porous as indicated by their densities. We therefore did not further characterize these compacts.

3.3. Hardness

The Knoop microhardness measured for compacts TJ01, TJ02, TJ03, and TJ04 using a load of 0.1 kg was approximately 3200 kg/mm^2. This value is similar to that measured for monolithic TiB_2 (3200–3400 kg/mm^2), and higher than that for monolithic TiC ($\approx$3000 kg/mm^2). This observation was expected since the compacts were richer in TiB_2 than TiC.

The effect of test load on the measured hardness was examined by increasing the load to 5 and 10 kg. The results are compared with those of monolithic TiB_2 and TiC in Fig. 5. When the test load was increased from 0.1 to 5 kg, the measured hardness decreased from $\approx$3200 to $\approx$1600 kg/mm^2. Further increases in the load did not result in significant further reductions in the
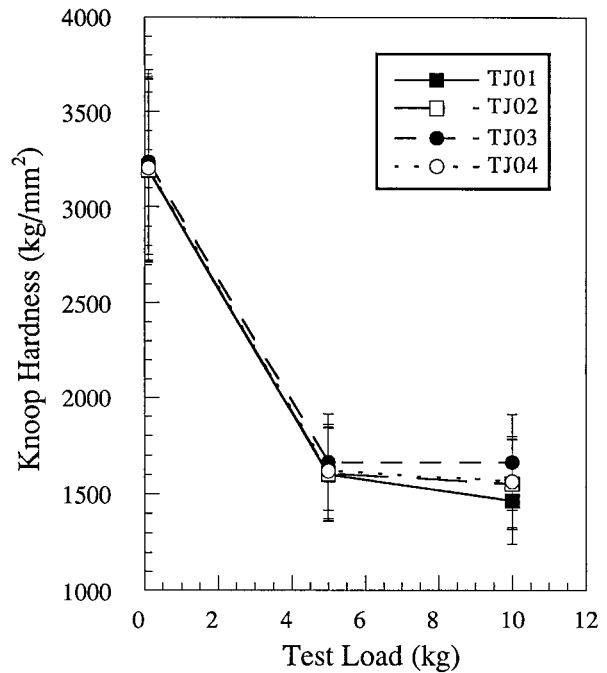
hardness. It is noted that the hardness of the TiB_2/TiC composites measured under loads of 5 and 10 kg were much higher than those of monolithic TiB_2 ($\approx$1200 kg/mm^2) and TiC ($\approx$1500 kg/mm^2). The hardness increase with higher loads indicates an improvement in grain boundary strength. It is believed that this strenthening mechanism is based on residual strain caused by shock wave induced defects.

4. Discussion

Physical properties of the TiB_2/TiC composites can be understood in terms of the adiabatic temperatures associated with the SHS process, and the increase in temperature and pressure during the dynamic compaction process. The delay time and C/M ratio determine the temperature increase during dynamic compaction. The temperature and pressure increases experienced during shock energy deposition to the SHS products were estimated for flyer plate velocities determined using the Gurney equation [14]. The assumptions used in making these estimates were that the TiB_2/TiC products were perfect mechanical mixtures of TiB_2 and TiC, and the product porosities were the same as those of the reactants. The actual temperature increase will be slightly higher than predicted because the shock energy deposition increases with increasing porosity and the product porosity is slightly higher than the reactant porosity due to dilation when the reaction is complete. The shock pressure will also be slightly lower than the predicted values but the differences should be negligible.

The impact velocities for C/M ratios of 0.6 and 0.3 were estimated to be 0.50 and 0.36 km/s, respectively. These low velocities probably would not cause significant differences in the shock energy and pressure for composites with TiB_2/TiC ratios of 2 : 1 and 1 : 2. The energy deposited for an impact velocity of 0.50 km/s and TiB_2/TiC ratios of 2 : 1 and 1 : 2 were

approximately 203 and 210 J/g, respectively. Assuming $C_v = 3R$, the corresponding temperature increase for the SHS reacted composites would be 538 and 532 °C, respectively. The energy is deposited at grain surfaces therefore the surface temperature will be much higher than temperatures at the grain centers. For the conditions employed, the surface temperature is expected to be more than 1500 °C higher than that at the grain centers [15]. Advani *et al.* [16] reported that the adiabatic temperature associated with the SHS production of TiC was in excess of 2200 K after 5–10 seconds of cooling. This suggested that during experiments described in this paper, the actual temperature at the grain surfaces following dynamic compaction would be higher than the melting temperatures of TiB_2 and TiC (3253 and 3340 K, respectively). Melting would result in fusion of the grains as indicated in Fig. 3. Melting and fusion of the grains is also expected for an impact velocity of 0.36 km/s. Energies deposited for an impact velocity of 0.36 km/s would be approximately 111 and 115 J/g for TiB_2/TiC ratios of 2 : 1 and 1 : 2, respectively. The corresponding temperature increases would be 294 and 290 °C, respectively. The shock pressure was estimated from the impedance mismatch of the Hugoniot of the flyer plate and the Hugoniot of the TiB_2/TiC mixtures. Shock pressure values for impact velocities of 0.50 and 0.36 km/s were approximately 1.41 and 0.77 GPa, respectively, as given in Fig. 6.

The key conclusion with respect to understanding mechanical properties of the TiB_2/TiC composites is that their grain surfaces were probably molten during compaction. The presence of liquid would improve consolidation of the material. Considering that the melting point of TiC is only 87 °C higher than that of TiB_2, one would expect properties for the TiC-rich composites to be similar to those for the TiB_2-rich materials. This, however, was not the observation suggesting the influence of other factors. Differences between densities of the composites may have been a consequence of their differing thermal expansion coefficients. The thermal expansion coefficients for TiB_2 and TiC are 4.6 and 7.95 × 10^{-6} K^{-1}, respectively, at 300–1300 K. The higher expansion coefficients associated with the TiC-rich composites may have resulted in higher thermal stresses and cracking as the composite cooled. This
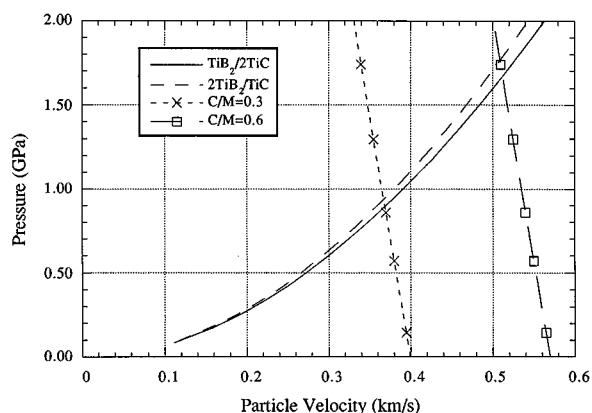
would cause the densities to be significantly lower than the theoretical values.

5. Summary
We have demonstrated the fabrication of TiB_2/TiC composites using a method based on self-propagating high temperature synthesis and subsequent dynamic compaction. These composites were fabricated from titanium and boron carbide powders. Preliminary estimates suggest that a 75% cost savings can be realized using boron carbide as a reactant instead of elemental boron and carbon. The TiB_2/TiC composite compacts were ~100 mm in diameter and 20 mm thick. Densities greater than 98% of the theoretical densities were achieved for compacts with TiB_2/TiC molar ratios of 2 : 1 while densities for compacts with 1 : 2 molar ratios were ~85%. The microhardness of the TiB_2-rich compacts were about 3200 kg/mm^2. This value is comparable to that for monolithic TiB_2 (3200–3400 kg/mm^2), and higher than that for monolithic TiC (3000 kg/mm^2). With further development the method described in this paper could be an economical way to produce fully-dense TiB_2/TiC composites.

References
1. E. K. STORMS, "The Refractory Carbides" (Academic Press, New York, 1967).
2. L. E. TOTH, "Transition Metal Carbides and Nitrides" (Academic Press, New York, 1971).
3. G. V. SAMSONOV and B. A. KOVENSKAYA, in "Boron and Refractory Borides," edited by V. I. Matkovich (Springer-Verlag, Berlin, 1977) p. 5.
4. Z. A. MUNIR and U. ANSELMI-TAMBURINI, *Mater. Sci. Reports* **3** (1989) 277.
5. Y. CHOI, M. E. MULLINS, K. WIJAYATILLEKE and J. K. LEE, *High Temp. Tech.* **3**(3) (1990) 227.
6. H. C. YI and J. J. MOORE, *J. Mater. Sci.* **25** (1990) 1159.
7. L. WANG, M. R. WIXOM and L. T. THOMPSON, *J. Mater. Sci.* submitted.
8. L. WANG, M. R. WIXOM and L. T. THOMPSON, Phase I Report to U.S. Army Ballistic Research Laboratory, DAAA15-91-C0088, 1993.
9. H. A. GREBE, Ph.D. thesis, New Mexico Tech, Socorro, New Mexico, 1993.
10. W. A. ZDANIESKI, *Am. Ceram. Soc. Bull.* **65** (1986) 1408.
11. D. R. STULL and H. PROPHET, "JANAF Thermodynamic Tables" (U.S. Department of Commerce, Washington, D.C., 1977).
12. J. W. McCAULEY, N. D. CORBIN, T. RESETAR and P. WONG, *Ceram. Eng. Sci. Proc.* **3**(9-10) (1982), 538.
13. M. I. MENDELSON, *J. Am. Ceram. Soc.* **52**(8) (1969) 443.
14. R. K. GURNEY, The Initial Velocities of Fragments from Bombs, Shells, and Grenades, BRL Report, 405, 1943.
15. I. SONG, Ph.D. thesis, New Mexico Tech, Socorro, New Mexico, 1992.
16. A. H. ADVANI, N. N. THADHANI, H. A. GREBE, R. HEAPS, C. COFFIN and T. KOTTKE, *J. Mater. Sci.* **27** (1992) 3309.
17. A. NIILER, L. J. KECSKES, T. KOTTKE, P. H. NETHERWOOD, Jr. and R. F. BENCK, Technical Report

Figure 6 Pressure and particle velocity curves for the TiB_2/TiC composites.

BRL-TR-2951, US Army Ballistic Research Laboratory, Aberdeen Proving Ground, MD, 1988.

18. M. A. RILEY and A. NIILER, Memorandum Report BRL-MR-3574, US Army Ballistic Research Laboratory, Aberdeen Proving Ground, MD, 1987.

19. A. NIILER, L. J. KECSKES and T. KOTTKE, in "Combustion and Plasma Synthesis of High Temperature Materials," edited by Z. A. Munir and J. B. Birch (VCH., New York, 1990) p. 309.

20. L. J. KECSKES, R. F. BENCK and P. H. NETHERWOOD, *J. Am. Ceram. Soc.* **73**(2) (1990) 383.

21. H. A. GREBE, A. ADVANI, N. N. THADHANI and T. KOTTKE, personal communication.